



# Projection of Light Pollution and Environmental Impact Estimation Based on Population and GDP: The Case of Türkiye

Research Article

10.65520/erciyesfen.1773264

## Imprint:

Volume: 42(1)

Year: 2026

Page: 259-276

Abdulvahap Yılmaz\*

Müjgan Elveren<sup>b</sup>

<sup>a</sup> Asst. Prof., Erzincan Binali Yıldırım  
University,

abdulvahap.yilmaz@erzincan.edu.tr

<sup>b</sup> Asst. Prof., Erzincan Binali Yıldırım  
University,

mujgan.elveren@erzincan.edu.tr

\* Corresponding Author

Received: 8/28/2025

Accepted: 1/11/2026

## Citation:

Abdulvahap Yılmaz, Müjgan Elveren  
(2026). Projection of Light Pollution  
and Environmental Impact

Estimation Based on Population and

GDP: The Case of Türkiye. *Erciyes*

*University Journal of Institute Of*

*Science and Technology*, 42(1), 259-

276.

[https://doi.org/10.65520/erciyesfen.](https://doi.org/10.65520/erciyesfen.1773264)

1773264

## Abstract

Abstract: Artificial Light at Night (ALAN) prediction can inform the development of strategies to minimise future light pollution and mitigate its adverse health, ecological, and environmental impacts. Population growth and GDP expansion significantly influence ALAN dynamics. This study quantifies changes in light pollution across Türkiye for 2012, 2017, and 2022, and predicts and maps potential changes in ALAN for 2027 and 2037 using the MOLUSCE plugin (MLP-ANN) in QGIS version 2.18, incorporating population and GDP as driving variables. The predicted and observed ALAN maps for 2022 show a satisfactory level of agreement, with an overall kappa coefficient of 0.63 and a general accuracy of 73.16%. The predicted and observed ALAN maps for 2022 exhibit an overall kappa coefficient of 0.63 and a general accuracy of 73.16%. Based on this validation, potential changes in ALAN according to Bortle classes were projected for 2027 and 2037. From 2022 onwards, ALAN intensity in the light suburban zone (20.1–19.1 mag/arcsec<sup>2</sup>) is projected to increase by 34,792.87 km<sup>2</sup>, while the suburban–urban transition zone (19.1–18 mag/arcsec<sup>2</sup>) is expected to expand by 2,979.80 km<sup>2</sup> by 2037. The predicted spatial patterns provide critical insights into future urbanisation trends and light pollution dynamics. The contraction of rural areas and expansion of suburban zones pose notable risks to environmental sustainability. Gains and losses among Bortle classes indicate that ALAN dynamics can be managed through spatial planning and that ALAN projections can serve as early-warning and scenario-based decision-support tools. Integrating ALAN maps into Environmental Impact Assessment (EIA) processes and spatial planning policies can help preserve dark-sky areas and mitigate the impacts of light pollution.

**Keywords:** Artificial Light at Night (ALAN), Bortle Scale, Environmental Sustainability, Remote Sensing Ecology



## Nüfus ve GSYİH'ye Dayalı Işık Kirliliğinin Projeksiyonu ve Çevresel Etki Tahmini: Türkiye Örneği

### Öz

ALAN (Gece Yapay Işık) tahmini, gelecekte ışık kirliliğini en aza indirmeye ve ışık kirliliğinin sağlık, ekolojik ve çevresel zararlarını azaltmaya yönelik stratejilerin geliştirilmesine katkıda bulunabilir. Nüfus ve GSYİH büyümesi, ALAN dinamikleri üzerinde önemli bir etkiye sahiptir. Bu çalışma, Türkiye'de ışık kirliliğindeki değişimleri 2012, 2017 ve 2022 yılları için ortaya koymayı; QGIS 2.18 yazılımında yer alan MOLUSCE eklentisi (MLP-ANN) ile nüfus ve GSYİH değişkenlerini kullanarak 2027 ve 2037 yıllarına yönelik olası ışık kirliliği değişimlerini tahmin etmeyi ve haritalamayı amaçlamaktadır. 2022

Screened by



Except where otherwise noted, content  
in this article is licensed under a  
Creative Commons 4.0 International  
license. Icons by Font Awesome.

yılına ait tahmini ve gerçek ALAN haritaları, 0.63'lük toplam kappa katsayısı ve %73.16'lık genel doğruluk değerine sahiptir. Bu doğrulama sonuçlarının ardından, 2027 ve 2037 yılları için Bortle sınıflarına göre ALAN'daki olası değişimler tahmin edilmiştir. 2022'den itibaren, hafif banliyö bölgesindeki (20.1-19.1) ALAN yükü 34792.87 km<sup>2</sup> artacak ve banliyö/kentsel geçiş bölgesindeki (19.1-18) ALAN yükü 2037 yılına kadar 2979.80 km<sup>2</sup> artacaktır. Tahmin edilen mekânsal değişimler, kentleşme ve ışık kirliliği dinamiklerinin gelecekteki eğilimlerine ilişkin önemli ipuçları sunmaktadır. Kırsal alanların daralması ve banliyölerin genişlemesi, çevresel sürdürülebilirlik açısından dikkat çekici riskler oluşturmaktadır. Borthle sınıfları arasındaki kayıp ve kazanımlar, ALAN dinamiklerinin planlama yoluyla yönlendirilebilir olduğunu ve ALAN projeksiyonlarının erken uyarı ve senaryo temelli bir karar destek aracı olarak kullanılabileceğini göstermektedir. Bu kapsamda, ALAN haritalarının ÇED süreçleri ve mekânsal planlama politikalarına entegre edilmesi, karanlık gökyüzü alanlarının korunmasına ve ışık kirliliğinin olumsuz etkilerinin azaltılmasına katkı sağlayacaktır.

**Anahtar kelimeler:** Gece Yapay Işık (ALAN), Bortle Ölçeği, Çevresel Sürdürülebilirlik, Uzaktan Algılama Ekoloji



## 1. Introduction

Light pollution is not only a problem that limits the visibility of the night sky, but also has a variety of negative effects on the environment and living organisms. This phenomenon, which is increasingly influenced by urbanization and industrialization, negatively affects ecological systems [1], wildlife behavior patterns [2], human health [3], and environmental processes on a larger scale [4].

One of the most obvious effects of light pollution is the disruption of the natural behavioral rhythms of flora and fauna [5]. It is scientifically proven that artificial light disrupts the circadian rhythms of nocturnal organisms, leading to changes in feeding, mating and migration behavior [5]; [6]. These disruptions negatively impact nocturnal pollinators, which threaten ecosystem health and play a critical role in agricultural productivity [7]. At the same time, artificial light has been observed to reduce predator-prey interactions [8] and disrupt the ecological balance [7]. In aquatic ecosystems, ALAN (Artificial Light At Night) complicates the dynamics between species within the habitat by affecting the behavioral responses of aquatic organisms [9]. It also poses a potential threat to molluscs [10].

The impact of light pollution on human health is also important. High levels of artificial lighting suppress melatonin production and cause sleep disturbances, anxiety and other emotional disorders [3]; [11]; [12]; [13]. However, chronic sleep disturbances have been shown to be associated with obesity, diabetes, cardiovascular disease [14] and certain cancers [12]; [15]; [16].

From an environmental perspective, light pollution reduces biodiversity and leads to a deterioration of ecosystem services [6]; [17]; [18]. Increased artificial brightness alters the natural habitats of various species and reduces their reproductive success. For example, many plants rely on certain light stimuli to flower and reproduce, while animals rely on darkness to protect themselves from predators [6]; [19]. In addition, insects, which are essential for agricultural productivity, become less active in bright environments, which can have a negative impact on agricultural production [18].

The relationship between light pollution and socio-economic factors is also striking. Artificial light exposure increases in areas with denser population and economic activities. Industrial and urbanized areas have the greatest problems with light pollution, especially at night [20]. Studies have shown that light pollution has a strong correlation with population ( $R_2=0.85$ ) and GDP ( $R_2=0.84$ ) (Aksaker et al., 2020) [21].

Public awareness of the health and environmental risks of light pollution is insufficient, which often leads to the negative consequences of light pollution being underestimated [13]; [16]. In this context, recognizing light pollution and raising awareness are crucial. Light pollution can be detected by ground-based and satellite-based measurements [22]. Satellite remote sensing data provides more holistic information as it covers large geographical areas. The Molusce plugin and Bortle classification

were used for the first time in the temporal and spatial analysis of light pollution in Italy [23].

This study aims to estimate the changes in light pollution in Turkey for the years 2027 and 2037 by using thematic ALAN layers divided into Bortle classes, GDP (Gross domestic product) and population density maps and the MOLUSCE plugin. This approach provides an innovative methodology that combines spatial analysis and modeling techniques to predict the future trajectory of light pollution.

## 2. Material and method

### 2.1 Study area

Turkey lies between 36–42° north latitude and 26–45° east longitude. 3% of the country's total area is on the European continent (Thrace), while the rest is on the Asian continent (Anatolia) (see **Figure 1**). With a total area of 783.568 km<sup>2</sup>, Turkey is one of the most populous countries in Europe with a population of around 85.33 million people. The average population density per square kilometer is around 111 people, and the annual population growth rate is given as 0.11% (TurkStat). In terms of total GDP, Turkey ranks sixth in the European Union [24]. According to the World Bank, Turkey is ranked 17th in the world economy [25]. In addition, the total amount of energy released into space by Turkey increased by 80% in 2019 compared to 2012 [26].



**Figure 1** Turkey's location in the world and the 2022 ALAN map.

### 2.2 Moluse plugin

MOLUSCE (Land Use Change Assessment Modules) is an innovative plugin developed for QGIS that can be used to estimate potential land cover changes. This tool, based on the Cellular Automata (CA) model, includes a transition probability matrix that is widely used by researchers [27];[28]. MOLUSCE supports four different algorithms: Multilayer Perceptron Artificial Neural Networks (MLP-ANN), Logistic Regression (LR), Multicriteria Evaluation (MCE) and Weight of Evidence (WoE). MOLUSCE was developed based on the CA-ANN model and contributes to the prediction of future land use scenarios by analyzing raster data on a pixel basis [29]; [30]; [31]. This model helps to determine spatial change processes by evaluating the initial data, the influence of neighboring cells and transition probabilities.

### 2.3 Data and Criteria

The datasets of the study include gross domestic product (GDP), population, and two thematic ALAN maps for the years 2017 and 2022. The ALAN maps were created using the thematic VNL annual layers of the Day-Night Band (DNB) of the Visible and Infrared Imaging Suite (VIIRS) (<https://eogdata.mines.edu/products/vnl/>). The population and GDP data are taken from the Turkish Statistical Institute datasets (<https://www.tuik.gov.tr/>). Detailed information on the source of the datasets can be found in **Table 1**.

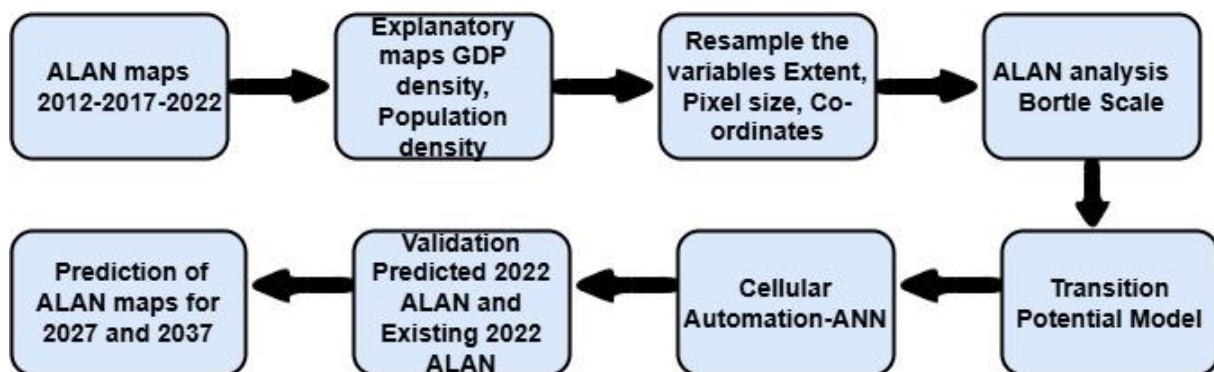
**Table 1** Source of the dataset maps.

Data	Criteria	ALAN simulation	Year	Description	Source	Data format
Light pollution	ALAN	Input maps	2012-2017-2022	NOAA-SUOMI-NPP-VIIRS/DNB spatial resolution 750 m	<a href="https://eogdata.mines.edu/products/vnl/">https://eogdata.mines.edu/products/vnl/</a>	.tif
Population	Population density	Special variable maps	2024	Address Based Population Registration System	<a href="https://data.tuik.gov.tr/">https://data.tuik.gov.tr/</a> Turkish Statistical Institute	.xls to .tif
GDP	GDP density	Special variable maps	2023	Gross Domestic Product by Province	<a href="https://data.tuik.gov.tr/">https://data.tuik.gov.tr/</a> Turkish Statistical Institute	.xls to .tif

To increase the accuracy of future projections, special variable maps can be used which are highly correlated with light pollution. Various studies have shown that GDP and population are closely linked to light pollution [6]; [32]. In this study, in addition to the three thematic area maps, GDP and population density maps were also created and included in the analysis process. The downloaded VIIRS/DNB maps were converted from  $nW/cm^2/sr$  to  $magnitude/arcsecond^2$  using the ArcGIS 10.8 infrastructure and basic formulas (see [33]). The converted thematic levels were classified according to the Bortle scale. Population and GDP data were downloaded in Excel format and linked to the GADM provincial map of the study area. Density maps were created with the ArcGIS Kernel Density Tool using provincial data values, and these data were converted to a classified raster format. Finally, all thematic maps were resized to the same cell size and prepared for analysis using the Molusce plugin in Quantum GIS 2.18.

## 2.4 Methods

The MOLUSCE plugin in Quantum GIS (QGIS) 2.18 uses the MLP-ANN learning process to predict changes in the input raster maps in the CA model and assess transition probabilities. The plugin performs future projections according to the procedure listed below [34]. The pixel-based model of MOLUSCE is based on the principle that each pixel is considered as an independent land unit in the raster data. This approach makes it possible to analyze spatial relationships and examine changes in land use at the local level in detail [35]. The flow chart of the study is presented in **Figure 2**.

**Figure 2** Flowchart of the methodology.

### 2.4.1 Inputs

In the first stage of the model, area maps are used for the initial year 2012 and the final year 2017. Population and GDP can be included as spatial variables in the model [36]; [37]. These factors are used to create a change map to analyze the patterns of change that occurred in the study area between 2012 and 2017 (see **Figure 3**). The descriptive maps are created in the same raster format in all datasets and extracted with the WGS 1984 geographic projection system with a pixel resolution of 50 meters. In the creation of the population and GDP density layers across Turkey, the city boundaries and total area are digitized from the GADM dataset, and the provincial population and GDP data are integrated and processed with the Kernel Density tool of ArcGIS Desktop 10.4.1 to convert them into density maps.

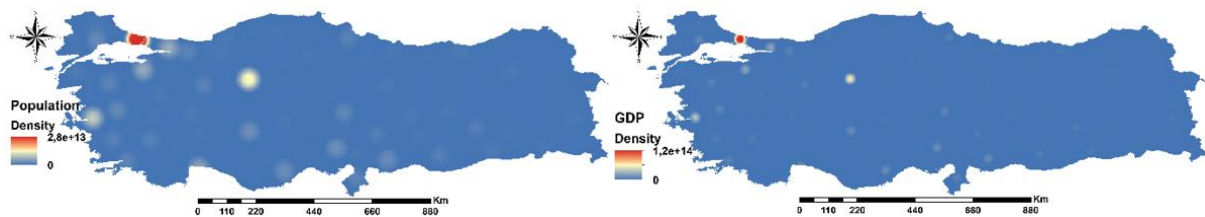


**Figure 3** Explanatory maps: GDP density and population density.

The MLP-ANN plugin is used to determine the change in area [38]; [39]. This plugin calculates the annual rate of area change over the selected period. MOLUSCE makes it possible to accurately determine the transitions between Bortle classes over time using a pixel-based method. The model generates transition probability matrices to predict future land cover changes by linking them to input parameters [40]; [41]. The transition probability matrix expresses the pixel rates of transformation from one class to another. In addition, thematic maps are created to reflect the changes in demographic and economic factors such as population and GDP between 2017 and 2022. Based on the current territorial patterns and change trends, spatial processes affecting thematic layers are modeled [42].

The study predicts the changes that will occur in the ALAN depending on the changes in the Bortle classes in 2027 and 2037 using classified raster images of the years 2017 and 2022 and 2017 and 2027.

### 2.4.2 Evaluation of the correlation

The MOLUSCE plugin uses common analysis methods such as Pearson correlation, Cramer coefficient and mutual information uncertainty to evaluate the relationship between raster maps and geographic variables [34]. The Cramer V coefficient quantifies this relationship with values between 0 and 1; a value of 1 indicates a strong association between raster maps and spatial determinants, while 0 indicates no relationship. Although these values do not provide definitive results, they give an impression of the applicability of transition potential modeling. In general, variables with a value above 0.1 are considered important for the assessment of transition potential [43].

### 2.4.3 Change area

This method uses thematic layers determined for the start and end year to calculate pixel-based changes over the relevant period and presents the results in the form of raster units, square kilometers and hectares [29]; [44]. The study used the ALAN maps for the years 2017-2022 and 2017-2027 as input data and calculated the area changes for these periods (see **Tables 5 and 6**).

### 2.4.4 Modeling the transition potential

The application is capable of using various methods such as MLP-ANN, Weights of Evidence (WoE), Logistic Regression (LR), and Multi-Criteria Evaluation (MCE) in the creation of potential transition maps [38]; [45]; [46]. In this study, the MLP-ANN method, which is widely preferred in the literature [28]; [47], was used to predict the ALAN map for the year 2022. The prediction accuracy and reliability of the MOLUSCE model can be verified using statistical methods such as kappa statistics and

confusion matrices [41]. In the study, the kappa coefficient was used to determine the accuracy of the ALAN maps generated.

#### 2.4.5 MLP-ANN

In the MOLUSCE application, the ALAN dataset can be effectively modeled with the combination of artificial neural networks (multilayer perceptron, MLP) and fuzzy logic techniques. The MLP model is a powerful method for pattern recognition and contributes to a better understanding of environmental changes. Supported by the application of the Markov chain, MLP can effectively analyze the changes that occur in the input maps [48]. Artificial neural networks (ANN) determine their usability by assigning values between 0 and 1 to the input maps using the fuzzy logic approach [28]. The basic elements of ANN are the interactions between interconnected neurons and the weight changes in these connections [49]. In this study, the following parameters were set for the estimation of ALAN maps: 1.000 iterations, 0.06 impulse value, 1-unit neighborhood, 0.001 learning rate, and 10 hidden layers [45]; [50]; [51].

#### 2.4.6 Validation

The kappa coefficient is an important statistical indicator that evaluates the degree of agreement of the predicted results with the real maps and gives an impression of the accuracy of the modeling process. This coefficient is a widely used method for measuring the similarity between the observed and predicted classifications. In the study, a forecast map for 2022 was created on the basis of the real ALAN maps from 2012 and 2017. The accuracy of this map was analyzed using the kappa coefficient by comparing it with the real map of 2022. The kappa coefficient was calculated using the formula given below [52]; [53].

$$Kappa = \frac{p_0 - p_e}{1 - p_e} \quad (1)$$

Here,  $p_0$  represents the observed compliance rate and  $p_e$  represents the expected compliance rate.

$$p_0 = \sum_{i=1}^c p_{ij} \quad (2)$$

$$p_e = \sum_{i=1}^c p_i T_j T_j \quad (3)$$

Where  $p_{ij}$  is the ratio of the cell in the  $i$ -th row and  $j$ -th column of the contingency table.  $p_i T_j$  is the sum of all cells in the  $i$ -th row of the contingency table.  $p_j T_i$  is the sum of all cells in the  $j$ -th column of the contingency table.  $c$  is the number of grid categories, i.e. the total number of different categories classified or evaluated.

The contingency table is used to determine the relationships between two variables and to evaluate the classification performance. In this study, each cell in the matrix numerically expresses how the raters agree or disagree on a particular category. Thus, it shows the agreement or differences in the evaluation criteria for each category [30].

To estimate the ALAN change map 2022, two spatial variables were combined and maps were simulated in which the factors of the spatial variables were integrated.

The analysis showed that the maximum kappa value of 0.63 and the maximum degree of accuracy of 73.16% were achieved for the combinations of population density, GDP density, and ALAN maps (**see Figure 4**). The maximum kappa value obtained was accepted as a good accuracy value in many studies [31]; [54]. Therefore, it was concluded that this combination has a satisfactory effect on the prediction of the classified ALAN maps. Subsequently, the ALAN map for 2027 and 2037 was predicted using the ALAN maps of 2017 and 2022 with the same combinations of spatial variables.



**Figure 4** Validation diagram between the observed 2022 ALAN map and the projected 2022 ALAN map.

### 2.5 Bortle Scale

The Bortle scale is an important astronomical measure that allows astronomers and astronomy enthusiasts to classify the night sky by its brightness and assess the suitability of the regions they will observe. This scale, first developed by John E. Bortle [55], consists of nine different levels, ranging from Class 1 (perfectly dark sky) to Class 9 (urban sky with heavy light pollution) [56].

This classification is based on observation criteria such as the Naked Eye Limiting Magnitude (NELM) for measuring the brightness of the night sky [57]. In a Class 1 region, observers can see stars up to a magnitude of +8 with the naked eye, while in urban areas, referred to as Class 8 and 9, visibility is severely limited by intense artificial light [57].

The Molusce plugin performs spatial analysis by focusing on pixel changes between classified thematic layers. In this study, the ALAN classes were created with reference to the Bortle scale, and all maps were categorized and colored according to the class boundaries in the Bortle scale (see Table 2).

The 2022 ALAN dataset contains 8 Bortle classes between 22.88-15.2 magnitude/arcsecond<sup>2</sup>, the 2017 ALAN dataset contains 6 Bortle classes between 21.48-15.34 magnitude/ arcsecond<sup>2</sup> and the 2017 ALAN dataset contains 5 Bortle classes between 21.11-15.31 magnitude/ arcsecond<sup>2</sup>. The Bortle classes between 22.88-20.8 magnitude/ arcsecond<sup>2</sup> in the 2022 ALAN dataset and the Bortle classes between 21.11-20.8 magnitude/ arcsecond<sup>2</sup> in the 2017 ALAN dataset were merged and reduced to a single class (rural/suburban transition). While this process neglects the analysis of Bortle classes lost between 2012 and 2022, it allows Molusce to make more effective predictions for the future as all input datasets are characterized by the same number of classes (5 classes).

**Table 2** Bortle Class and Sky Brightness Table.

Color	Bortle	Sky Brightness	Sky Class
Magnitude	Class	Mag/Arcsecond <sup>2</sup>	
	1	>21.9	Perfect (Excellent) sky
	2	21.9-21.5	Typical dark sky
	3	21.5-21.3	Rural sky
	4	21.3-20.8	Rural/suburban transition
	4.5	20.8-20.1	Suburban
	5	20.1-19.1	Light(Bright) suburban
	6.7	19.1-18	Suburban/urban transition
	8.9	<18	City Sky

### 3. Results and discussion

**Table 3** shows the probability matrix of change in ALAN classes from 2012 to 2017. The values in the table range from 0 to 1, with values closer to 1 representing larger changes. However, the diagonal cells are an exception, showing no change because they are in the same class.

**Table 3** Changes in the ALAN probability matrix between 2012 and 2017.

Year	2017					
	<b>Sky Brightness Mag/Arcsec<sup>2</sup></b>	21.3-20.8	20.8-20.1	20.1-19.1	19.1-18	<18
<b>2012</b>	21.3-20.8	0.602909	0.381680	0.014652	0.000688	0.000071
	20.8-20.1	0.011180	0.449557	0.526550	0.011539	0.001173
	20.1-19.1	0.003774	0.044276	0.697345	0.246886	0.007720
	19.1-18	0.001593	0.006155	0.053793	0.727327	0.211133
	<18	0.000214	0.000444	0.001545	0.041356	0.956442

The change trend of ALAN from 2012 to 2022 is shown in **Table 4** and **Table 5** shows the ALAN analysis for each of the five years. **Figure 5** shows the spatial change of ALAN from 2012 to 2022. In 2012, the (21.3-20.8) Rural/Suburban transition class accounted for 78.26% of the total area, followed by (20.8-20.1) Suburban 11.79%, (20.1-19.1) Light Suburban 6.62%, (19.1-18) Suburban/ Urban transition 2.04%, (<18) City Sky 1.3%. It was found that the trend for all ALAN classes changed between 2012, 2017, and 2022. Compared to 2012, in 2022, (21.3-20.8) Rural/Suburban Transition decreased by 58.8%, while (20.8-20.1) Suburban, (20.1-19.1) Light Suburban, (19.1-18) Suburban/ Urban Transition, and (<18) City Sky increased by 45.08%, 10.3%, 2.62%, and 0.82%, respectively. This change in the classes of light pollution is related to many anthropogenic, atmospheric changes, and the main reason for this is the increase in population by 13.03% and the increase in GDP per capita by %833 in TL in Turkey <sup>1</sup> from 2012 to 2022. These values reveal that the spatial reflection of economic growth accelerates the transformation of ALAN classes through more intense lighting and suburbanisation. Furthermore, the significant change in Rural/Suburban Transition areas between 2012 and 2022 (21.3–20.8) is of a scale that cannot be explained solely by natural urbanisation dynamics and can be associated with the administrative inclusion of rural areas into the urban system by Law No. 6360 [58]. Indeed, the examples of Samsun and Konya show that the transformation of villages into neighbourhood status accelerates the "forced urbanisation" process by effectively opening rural spaces to urban use [59].

**Table 4** Analysis of ALAN from 2012 to 2022. % indicates what percentage of the total surface area of the classroom it covers.

Sky Brightness Mag/Arcsec <sup>2</sup>	2012 km <sup>2</sup>	%	2017 km <sup>2</sup>	%	2022 km <sup>2</sup>	%
21.3-20.8	624228.17	78.26	375832.07	47.11	155078.47	19.44
20.8-20.1	94066.20	11.79	285582.04	35.80	453618.51	56.87
20.1-19.1	52776.77	6.62	96110.35	12.05	134981.15	16.92
19.1-18	16265.64	2.04	26286.41	3.30	37152.83	4.66
<18	10333.12	1.30	13895.85	1.74	16875.19	2.12

<sup>1</sup> <https://data.tuik.gov.tr/>

**Table 5** ALAN analysis for each of the five years from 2012 to 2022.

Sky Brightness Mag/Arcsec <sup>2</sup>	2012-2017		2017-2022	
	km <sup>2</sup>	% Changes	km <sup>2</sup>	% Changes
21.3-20.8	-248396.10	-31.14	-220753.60	-27.67
20.8-20.1	191515.83	24.01	168036.47	21.06
20.1-19.1	43333.57	5.43	38870.81	4.87
19.1-18	10020.77	1.26	10866.42	1.36
<18	3562.72	0.45	2979.34	0.37

**Table 5** shows that the increase in suburban (20.8–20.1) areas (168,036 km<sup>2</sup>) during the 2017–2022 period maintained its momentum from the previous period. This trend can be attributed to reverse migration during the pandemic [60] and the shift towards low-density settlements after the earthquake [61]; [62], in addition to structural urbanisation dynamics. Thus, we believe that suburbanisation has accelerated under the influence of forced spatial mobility.

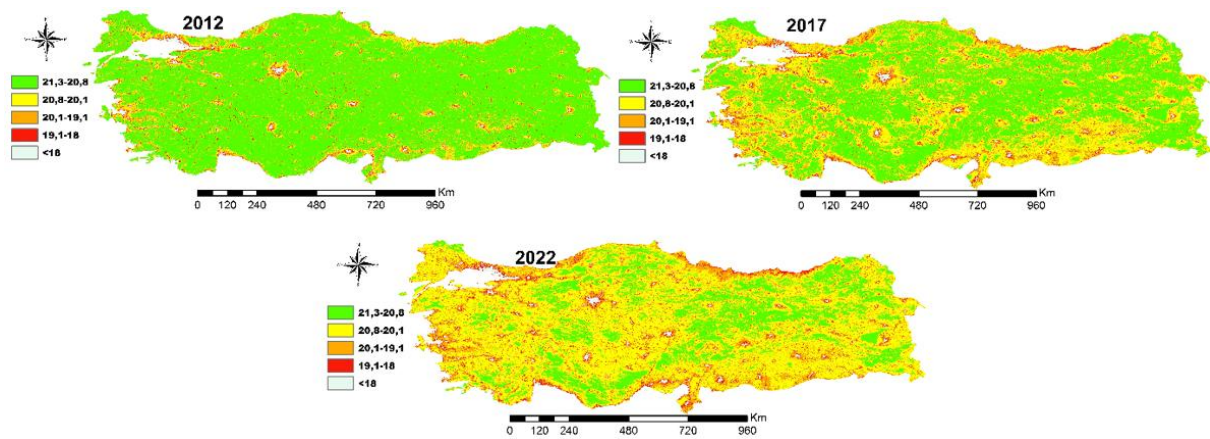


**Figure 5** maps of the ALAN for the years 2012, 2017, 2022.

**Table 6** shows the changes in the ALAN categories between 2022 and 2027. It can be seen that the Light Suburban (20.1-19.1) and Suburban/Urban Transition (19.1-18) classes can increase by 26209.79 km<sup>2</sup> and 19.33 km<sup>2</sup> respectively, while the Rural/Suburban Transition (21.3-20.8), Suburban (20.8-20.1) and City Sky (<18) classes can decrease by 961.42 km<sup>2</sup>, 25260.94 km<sup>2</sup> and 6.75 km<sup>2</sup> respectively. In addition, the changes in the classified ALAN classes are analyzed as a percentage of the total area of the study area boundaries. Positive values indicate that the ALAN class has improved, while negative values indicate a deterioration of the class.

**Table 6** Distribution of ALAN categories between 2022 and 2027.

Sky Brightness Mag/Arcsec <sup>2</sup>	2022 (km <sup>2</sup> )	2027 (km <sup>2</sup> )	Change (km <sup>2</sup> )	Area in % 2022	Area in % 2027	Percentage change (2022-2027)
21.3-20.8	155078.47	154117.05	-961.42	19.44	19.32	-0.12
20.8-20.1	453618.51	428357.56	-25260.94	56.87	53.70	-3.17
20.1-19.1	134981.15	161190.94	26209.79	16.92	20.21	3.29
19.1-18	37152.83	37172.16	19.33	4.66	4.66	0.00
<18	16875.19	16868.44	-6.75	2.12	2.11	0.00

**Table 7** shows how the ALAN classification could change between 2022 and 2037. By 2037, an increase in the area of influence of 34792.87 km<sup>2</sup> and 2979.80 km<sup>2</sup> is observed for the light suburban (20.1-19.1) and transitional Suburban/Urban (19.1-18) categories, respectively. A decrease in impact of 5408.84 km<sup>2</sup>, 32076.01 km<sup>2</sup> and 287.83 km<sup>2</sup> is projected for the rural/suburban transition (21.3-20.8), suburban (20.8-20.1) and City Sky (<18), respectively. **Figure 6** shows the expected ALAN changes in 2027 and 2037.

**Table 7** Distribution of ALAN categories between 2022 and 2037.

Sky Brightness Mag/Arcsec <sup>2</sup>	2022 (km <sup>2</sup> )	2037 (km <sup>2</sup> )	Change (km <sup>2</sup> )	Area in % 2022	Area in % 2037	Percentage change (2022-2037)
21.3-20.8	155078.47	149669.63	-5408.84	19.44	18.76	-0.68
20.8-20.1	453618.51	421542.50	-32076.01	56.87	52.84	-4.02
20.1-19.1	134981.15	169774.02	34792.87	16.92	21.28	4.36
19.1-18	37152.83	40132.63	2979.80	4.66	5.03	0.37
<18	16875.19	16587.36	-287.83	2.12	2.08	-0.04

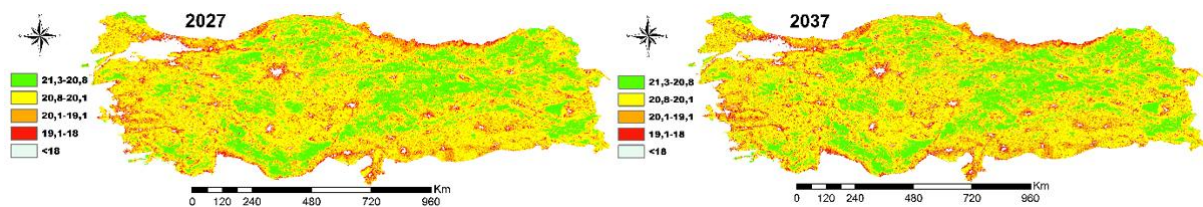


**Figure 6** Projected ALAN maps for 2027 and 2037.

Between 2022 and 2037, the percentage difference in ALAN classes decreased by 0.68% for Rural/Suburban Transition (21.3-20.8), by 4.02% for Suburban (20.8-20.1), and by 0.04% for City Sky (<18), while the other categories of Light Suburban (20.1-19.1) and Suburban/Urban Transition (19.1-18) increased by 4.36% and 0.37%, respectively. The analysis showed that the loss of area in one class led to an increase in area in another class and that the percentage area gains and losses by class transition were balanced.

Tables 4 and 7 show that suburban areas (20.8-20.1) increased by 45.08% during the 2012-2022 period, and that the light suburban class is projected to expand by 34,792 km<sup>2</sup> by 2037. This trend aligns with the leapfrog development model observed in cities such as Ankara, Konya, and Samsun [58];[59]; [63]; [64]; [65], and indicates that suburban classes are growing faster than urban cores, with new settlements and lighting centres forming on city outskirts.

Table 7 predicts a contraction in the “City Sky” (<18) class and that suburbanisation will become the dominant spatial form by 2037. This prediction is consistent with TÜİK population projections, population momentum<sup>2</sup>, and the economic pressure on city centres [66]. We suggest that the approximately 34,000 km<sup>2</sup> increase in suburban areas, driven by population displacement to lower-cost suburban zones on the periphery, could be a spatial reflection of demographic and economic congestion.

Most studies investigating the effects of ALAN on ecosystems have focused on impacts at the level of individual organisms. These studies encompass a wide range of biological responses, including gene expression, physiology, feeding behavior, diel activity patterns, migration, and reproductive behaviors [67]. For example, one experimental study demonstrated that exposure to artificial light acts as a stressor that alters gene expression levels in mice [68]. In another study, it was shown that by disrupting natural light regimes, masking natural environmental cues, and providing misleading

<sup>2</sup> <https://data.tuik.gov.tr/Bulten/Index?p=Nufus-Projeksiyonlari-2023-2100-53699>

information, ALAN can impair visual perception and biological rhythms, thereby altering the natural behaviors and activity patterns of nocturnal insects [69].

These data show that, as a natural consequence of the urbanization process, more and more rural areas are gradually becoming more densely populated. In the course of urban sprawl, suburban areas gain space from rural areas, while dense suburbs become City Skys. As a result, the class transitions even out and the total area lost reappears as area gained in another category. This trend can provide urban planners with important data for the development of sustainable growth strategies.

### **3.1 Solution**

The estimation of ALAN can contribute to the development of strategies to minimize light pollution in the future. MLP-ANN was used to simulate and predict classified ALAN maps in Turkey. Two spatial variable factors, namely population and GDP density, had a significant impact on the estimation and simulation process of the country's ALAN maps. The kappa value of 0.63 indicates the highest degree of accuracy between the actual and predicted ALAN maps of 2022.

The ALAN maps for 2027 and 2037 were created based on the ALAN maps for 2012 and 2017 using the combinations of spatial variable factors. From 2022, the ALAN burden in the slightly suburban region (20.1-19.1) will increase by 34792.87 km<sup>2</sup>, and the ALAN burden in the suburban/Urban transition region (19.1-18) will increase by 2979.80 km<sup>2</sup> by 2037. In the rural/suburban transition (21.3-20.8), suburban (20.8-20.1), and city center (<18) categories, the impact is predicted to decrease by 5408.84 km<sup>2</sup>, 32076.01 km<sup>2</sup>, and 287.83 km<sup>2</sup> respectively. The projected spatial changes provide important indications of how urbanization and the dynamics of light pollution will develop in the future. In particular, the shrinking of rural areas and the expansion of suburbs pose considerable risks to environmental sustainability.

#### **3.1.1 Expected environmental impact**

The observed shrinkage of the Rural/Suburban Transition class (21.3–20.8) is likely to reflect the progressive conversion of rural landscapes into residential and semi-urban land uses. This transformation may result in the loss of agricultural land, leading to reduced food production capacity and increased pressure on remaining arable areas. In addition to economic consequences for rural communities, the decline in agricultural land may also disrupt ecosystem services such as soil fertility, water regulation, and carbon sequestration, thereby negatively affecting biodiversity and landscape sustainability.

The continued expansion of suburban areas, particularly within the light suburban and suburban/urban transition classes, is expected to intensify habitat fragmentation across forested and semi-natural environments. Habitat fragmentation can reduce habitat connectivity, limit species dispersal, and increase edge effects, ultimately leading to population declines in sensitive species. Such changes may alter trophic interactions, reduce genetic diversity, and compromise the long-term resilience of local ecosystems, posing significant threats to native flora and fauna.

Urban sprawl associated with suburban expansion is also expected to influence transportation patterns and energy consumption. Reduced accessibility to public transportation systems and increased dependence on private vehicles may lead to higher fossil fuel consumption, elevated greenhouse gas emissions, and intensified contributions to climate change. Furthermore, the conversion of vegetated and permeable surfaces into built-up areas is likely to exacerbate the loss of green spaces, resulting in diminished air quality, reduced carbon uptake, and increased surface and air temperatures. These changes may intensify the urban heat island effect, elevate energy demand for cooling, and adversely affect both environmental quality and human well-being.

Collectively, these processes highlight the potential for long-term environmental degradation driven by land-use transitions, emphasizing the need for sustainable spatial planning strategies that balance urban development with the conservation of agricultural lands, natural habitats, and ecosystem services.

### 3.1.2 Proposed solutions

Compact and sustainable urban planning should be pursued, and multi-story, densely populated areas should be encouraged instead of irregular suburbanization. Cities should be expanded by creating green corridors and ecological connections.

Special protection zones should be established to protect agricultural and forest areas and development in these areas should be restricted. The public transport infrastructure should be strengthened and new suburban areas should be integrated into the public transport system.

Dependence on private transport should be reduced, and energy-efficient lighting technologies (e.g., low-spectral impact and directional LED systems) should be made mandatory.

Special protection zones should be established to limit the ecological impact of the ALAN, restrict lighting standards in rural areas, and implement planning decisions that preserve rural character.

The inter-class land losses and gains identified in the study demonstrate that ALAN dynamics can be managed through planning, and show that ALAN projections can serve as an early warning and scenario-based decision support tool for planning authorities. In this context, it is recommended that ALAN maps be integrated into environmental impact assessment (EIA) processes, master plans, and regional development strategies. This recommendation can help ensure the preservation of areas that maintain dark-sky conditions (21.3–20.8 mag/arcsec<sup>2</sup>) for future generations and mitigate the adverse impacts of ALAN.

### 3.1.3 Limitations of the Model

MOLUSCE, due to its simulation logic based solely on integer multiples of time differences between two dates, cannot represent continuity in the intervening years and, because its structure is based on past trends, cannot predict sudden breaks that may occur in the future, such as rapid economic changes, planning interventions, or disasters [70];[71].

Furthermore, as this study represents the dynamics of artificial light distribution only through macro-scale drivers such as population growth and GDP per capita, multidimensional factors influencing artificial light distribution (such as planning policies, infrastructure, technological changes, and local astrometeorological and atmospheric conditions) are excluded from the model's scope. Future research should enhance the explanatory power and spatial sensitivity of artificial light distribution by integrating these variables into a multi-criteria or hybrid modelling framework.

## 4. Conclusion

- The estimation and simulation of ALAN using MLP-ANN models, based on spatial factors such as population and GDP density, can provide valuable insights for urban planning and light pollution management.
- The kappa accuracy value of 0.63 and an overall accuracy rate of 73.16% between actual and predicted ALAN maps for 2022 demonstrate the model's reliability.
- The 2037 projections reveal that ALAN exposure will increase in suburban zones and decrease in rural and city center areas, indicating urban sprawl, rural shrinkage, and growing risks to environmental sustainability.
- The transformation of rural areas and suburban expansion may lead to agricultural loss, habitat fragmentation, and a decline in biodiversity.
- Current evidence indicates that light pollution has become an increasingly urgent environmental issue threatening ecological security. Given the practical indispensability of ALAN, it is recommended that strategies be developed to minimize its adverse effects on ecosystems.
- In particular, the spatial deployment of ALAN should be planned in accordance with ecological

sensitivities, while limitations on light intensity, duration, and spectral composition, along with the implementation of effective regulatory and monitoring frameworks, are essential for mitigating the ecological impacts of light pollution.

- The inter-class land losses and gains identified in the study demonstrate that ALAN dynamics can be managed through planning, and show that ALAN projections can serve as an early warning and scenario-based decision support tool for planning authorities.
- In this context, it is recommended that ALAN maps be integrated into environmental impact assessment (EIA) processes, master plans, and regional development strategies. This recommendation can help ensure the preservation of areas that maintain dark-sky conditions (21.3–20.8 mag/arcsec<sup>2</sup>) for future generations and mitigate the adverse impacts of ALAN.



**Peer-review:** External, Independent.

**Acknowledgements:**

-

**Declarations:**

**1. Statement of Originality:**

This work is original.

**2. Author Contributions:**

**Concept:** AY; **Conceptualization:** AY; **Literature Search:** AY,ME; **Data Collection:** AY; **Data Processing:** AY; **Analysis:** AY,ME; **Writing – original draft:** AY,ME; **Writing – review & editing:** AY,ME.

**3. Ethics approval:**

Not applicable.

**4. Funding/Support:**

This work has not received any funding or support.

**5. Competing Interests:**

The authors declare no competing interests.

**6. GenAI Usage Statement:**

No GenAI tools were used at any stage of the study.

**7. Sustainable Development Goals:**



**REFERENCES**

- [1] Hao, Q., Wang, L., Liu, G., Ren, Z., Wu, Y., Yu, Z., & Yu, J. (2023). Exploring the construction of urban artificial light ecology: a systematic review and the future prospects of light pollution. *Environmental Science and Pollution Research*, 30(46), 101963-101988.
- [2] Wise, S. (2007). Studying the ecological impacts of light pollution on wildlife: amphibians as

- models. *Starlight: A Common Heritage*; Cipriano, M., Jafar, J., Eds, 209-218.
- [3] Lu, J., Zou, R., Yang, Y., Bai, X., Wei, W., Ding, R., & Hua, X. (2024). Association between nocturnal light exposure and melatonin in humans: a meta-analysis. *Environmental Science and Pollution Research*, 31(3), 3425-3434.
- [4] Kim, K. H., Choi, J. W., Lee, E., Cho, Y. M., & Ahn, H. R. (2015). A study on the risk perception of light pollution and the process of social amplification of risk in Korea. *Environmental Science and Pollution Research*, 22, 7612-7621
- [5] Fauzia, A. (2024). The impact of Artificial Light at Night (ALAN) on biodiversity: flora and fauna at Kebun Raya Bogor. *Ecotourism and Environment Conservation*, 1(2).
- [6] Falchi, F., Furgoni, R., Gallaway, T. A., Rybnikova, N. A., Portnov, B. A., Baugh, K., ... & Elvidge, C. D. (2019). Light pollution in USA and Europe: The good, the bad and the ugly. *Journal of environmental management*, 248, 109227.
- [7] Falchi, F., Cinzano, P., Elvidge, C., Keith, D., & Haim, A. (2011). Limiting the impact of light pollution on human health, environment and stellar visibility. *Journal of Environmental Management*, 92(10), 2714-2722.
- [8] Tamir, R., Lerner, A., Haspel, C., Dubinsky, Z., & Iluz, D. (2017). The spectral and spatial distribution of light pollution in the waters of the northern Gulf of Aqaba (Eilat). *Scientific reports*, 7(1), 42329.
- [9] Jechow, A., & Hölker, F. (2019). How dark is a river? Artificial light at night in aquatic systems and the need for comprehensive night-time light measurements. *Wiley Interdisciplinary Reviews: Water*, 6(6), e1388.
- [10] Hussein, A. A., Bloem, E., Fodor, I., Baz, E. S., Tadros, M. M., Soliman, M. F., ... & Koene, J. M. (2021). Slowly seeing the light: an integrative review on ecological light pollution as a potential threat for mollusks. *Environmental Science and Pollution Research*, 28, 5036-5048.
- [11] Navara, K.J. and Nelson, R.J. (2007) The dark side of light at night: physiological, epidemiological, and ecological consequences. *Journal of Pineal Research*, 43(3), 215–224.
- [12] Argys, L., Averett, S., & Yang, M. (2020). Light pollution, sleep deprivation, and infant health at birth. *Southern Economic Journal*, 87(3), 849-888.
- [13] Menculini, G., Cirimbilli, F., Raspa, V., Scopetta, F., Cinesi, G., Chieppa, A., ... & Tortorella, A. (2024). Insights into the effect of light pollution on mental health: focus on affective disorders—a narrative review. *Brain Sciences*, 14(8), 802.
- [14] Minnetti M, Hasenmajer V, Pofi R, et al. Fixing the broken clock in adrenal disorders: focus on glucocorticoids and chronotherapy. *J Endocrinol*. 2020;246(2):R13–R31. doi: 10.1530/JOE-20-0066 ; Münzel, T., Hahad, O., & Daiber, A. (2021). The dark side of nocturnal light pollution. Outdoor light at night increases risk of coronary heart disease. *European Heart Journal*, 42(8), 831-834.
- [15] Abdraboh, M. E., El-Missiry, M. A., Othman, A. I., Taha, A. N., Elhamed, D. S. A., & Amer, M. E. (2022). Constant light exposure and/or pinealectomy increases susceptibility to trichloroethylene-induced hepatotoxicity and liver cancer in male mice. *Environmental Science and Pollution Research*, 29(40), 60371-60384.
- [16] Tang, L. (2013). Light at night: a new kind of environment pollution. *Advanced Materials Research*, 807-809, 636-640.
- [17] Warrant, E.; Frost, B.; Green, K.; Mouritsen, H.; Dreyer, D.; Adden, A.; Brauburger, K.; Heinze, S. The Australian Bogong Moth *Agrotis Infusa*: A Long-Distance Nocturnal Navigator. *Front. Behav.*

- Neurosci. 2016, 10, 77.
- [18] Anderson, S., Kubiszewski, I., & Sutton, P. (2024). The ecological economics of light pollution: impacts on ecosystem service value. *Remote Sensing*, 16(14), 2591. <https://doi.org/10.3390/rs16142591>
- [19] Falcón, J., Torriglia, A., Attia, D., Viénot, F., Gronfier, C., Behar-Cohen, F., ... & Hicks, D. (2020). Exposure to artificial light at night and the consequences for flora, fauna, and ecosystems. *Frontiers in Neuroscience*, 14, 602796.
- [20] Górniak-Zimroz, J., Romańczukiewicz, K., Sitarska, M., & Szrek, A. (2024). Light-pollution-monitoring method for selected environmental and social elements. *Remote Sensing*, 16(5), 774.
- [21] Aksaker, N., Yerli, S. K., Kurt, Z., Bayazit, M., Aktay, A., & Erdoğan, M. A. (2020). A case study of light pollution in France. *Astrophysics and Space Science*, 365(9), 153.
- [22] Yılmaz, A. (2024) Işık Kirliliği Tespitinde Uzay ve Yer Ölçüm Yöntemleri ve Türkiye Perspektifinde Sistemik İnceleme. *Turkish Journal of Astronomy and Astrophysics*, 5(2), 22-27. <https://doi.org/10.55064/tjaa.1449416>
- [23] Yılmaz, A. (2025). Temporal and Spatial Analysis of Light Pollution Changes: A Case Study of Italy. *Astronomische Nachrichten*, e70041.
- [24] Derviş, K. (2013). Turkey and Europe, a New Perspective. *Global Turkey in Europe*, 39, 21.
- [25] Tuna, K., Kayacan, E., & Bektaş, H. (2015). The relationship between research & development expenditures and economic growth: The case of Turkey. *Procedia-Social and Behavioral Sciences*, 195, 501-507.
- [26] Yerli, S. K., Aksaker, N. A. Z. I. M., Bayazit, M., Kurt, Z., Aktay, A. L. İ. Ş. A. N., & Erdoğan, M. A. (2021). The temporal analysis of light pollution in Turkey using VIIRS data. *Astrophysics and Space Science*, 366(4), 34.
- [27] NextGIS (2017) MOLUSCE-quick and convenient aanalysis of LandCoverChanges. <https://nextgis.com/blog/molusce/> (accessed 05 March 2025).
- [28] Kamaraj, M., & Rangarajan, S. (2022). Predicting the future land use and land cover changes for Bhavani basin, Tamil Nadu, India, using QGIS MOLUSCE plugin. *Environmental Science and Pollution Research*, 29(57), 86337-86348.
- [29] Rahman, M. T. U., Tabassum, F., Rasheduzzaman, M., Saba, H., Sarkar, L., Ferdous, J., ... & Zahedul Islam, A. Z. M. (2017). Temporal dynamics of land use/land cover change and its prediction using CA-ANN model for southwestern coastal Bangladesh. *Environmental monitoring and assessment*, 189, 1-18.
- [30] Saputra, M. H., & Lee, H. S. (2019). Prediction of land use and land cover changes for North Sumatra, Indonesia, using an artificial-neural-network-based cellular automaton. *Sustainability*, 11(11), 3024.
- [31] Aneesha Satya, B., Shashi, M., & Deva, P. (2020). Future land use land cover scenario simulation using open source GIS for the city of Warangal, Telangana, India. *Applied Geomatics*, 12(3), 281-290.
- [32] Levin, N., & Zhang, Q. (2017). A global analysis of factors controlling VIIRS nighttime light levels from densely populated areas. *Remote sensing of environment*, 190, 366-382.
- [33] Yılmaz, A. (2024). ESTIMATION OF ENERGY LOSS DUE TO LIGHT POLLUTION USING SATELLITE AND FIELD MEASUREMENT DATA: EXAMPLE OF ERZİNCAN CITY. *Environmental Engineering & Management Journal (EEMJ)*, 23(12).

- [34] Hakim, A. M. Y., Baja, S., Rampisela, D. A., & Arif, S. (2019, June). Spatial dynamic prediction of landuse/landcover change (case study: tamalanrea sub-district, makassar city). In IOP Conference Series: Earth and Environmental Science (Vol. 280, No. 1, p. 012023). IOP Publishing.
- [35] Abbas, Z., Yang, G., Zhong, Y., & Zhao, Y. (2021). Spatiotemporal change analysis and future scenario of LULC using the CA-ANN approach: A case study of the greater bay area, china. *Land*, 10(6), 584.
- [36] Gao, C., Cheng, D., Iqbal, J., & Yao, S. (2023). Spatiotemporal change analysis and prediction of the great yellow river region (GYRR) land cover and the relationship analysis with mountain hazards. *Land*, 12(2), 340.
- [37] Kavhu, B., Mashimbye, Z. E., & Luvuno, L. (2022). Characterising social-ecological drivers of landuse/cover change in a complex transboundary basin using singular or ensemble machine learning. *Remote Sensing Applications: Society and Environment*, 27, 100773.
- [38] Buğday, E., & Buğday, S. E. (2019). Modeling and simulating land use/cover change using artificial neural network from remotely sensing data. *Cerne*, 25, 246-254.
- [39] Msovu, U. E., Mulungu, D. M., Nobert, J. K., & Mahoo, H. (2019). Land use/cover change and their impacts on streamflow in Kikuletwa Catchment of Pangani River Basin, Tanzania. *Tanzania Journal of Engineering and Technology*, 38(2), 171-192.
- [40] Alshari, E. A., and Gawali, B. W. 2022. Modeling Land Use Change in Sana'a City of Yemen with MOLUSCE. *Journal of Sensors Hindawi Limited 2022*: 1–15. DOI: 10.1155/2022/7419031.
- [41] Iskandar, B., Kurnia, A. A., Jauhari, A., & Zannah, F. (2024). Modeling Land Cover Change Using MOLUSCE in Kahayan Tengah Forest Management Unit, Kalimantan Tengah. *Jurnal Sylva Lestari*, 12(2), 242-257.
- [42] Lukas, P., Melesse, A. M., and Kenea, T. T. 2023. Prediction of Future Land Use/Land Cover Changes Using A Coupled CA-ANN Model in the Upper Omo–Gibe River Basin, Ethiopia. *Remote Sensing* 15(4): 1148.
- [43] Muhammad, R., Zhang, W., Abbas, Z., Guo, F., & Gwiazdzinski, L. (2022). Spatiotemporal change analysis and prediction of future land use and land cover changes using QGIS MOLUSCE plugin and remote sensing big data: a case study of Linyi, China. *Land*, 11(3), 419.
- [44] Ashaolu, E. D., Olorunfemi, J. F., & Ifabiyi, I. P. (2019). Assessing the spatio-temporal pattern of land use and land cover changes in Osun drainage basin, Nigeria. *Journal of Environmental Geography*, 12(1-2), 41-50.
- [45] El-Tantawi, A. M., Bao, A., Chang, C., & Liu, Y. (2019). Monitoring and predicting land use/cover changes in the Aksu-Tarim River Basin, Xinjiang-China (1990–2030). *Environmental monitoring and assessment*, 191, 1-18.
- [46] Guidigan, M. L. G., Sanou, C. L., Ragatoa, D. S., Fafa, C. O., & Mishra, V. N. (2019). Assessing land use/land cover dynamic and its impact in Benin Republic using land change model and CCI-LC products. *Earth Systems and Environment*, 3(1), 127-137.
- [47] Baghel, S., Kothari, M. K., Tripathi, M. P., Singh, P. K., Bhakar, S. R., Dave, V., & Jain, S. K. (2024). Spatiotemporal LULC change detection and future prediction for the Mand catchment using MOLUSCE tool. *Environmental Earth Sciences*, 83(2), 66.
- [48] Shen, L., Li, J. B., Wheate, R., Yin, J., & Paul, S. S. (2020). Multi-layer perceptron neural network and Markov chain based geospatial analysis of land use and land cover change. *J. Environ. Inform. Lett*, 3, 29-39.
- [49] Bhattacharyya, S., Sarkar, D., Roy, R., Chakraborty, S., Goel, V., & Almatrafi, E. (2021). Application

- of new artificial neural network to predict heat transfer and thermal performance of a solar air-heater tube. *Sustainability*, 13(13), 7477.
- [50] Perović, V., Jakšić, D., Jaramaz, D., Koković, N., Čakmak, D., Mitrović, M., & Pavlović, P. (2018). Spatio-temporal analysis of land use/land cover change and its effects on soil erosion (Case study in the Oplenac wine-producing area, Serbia). *Environmental monitoring and assessment*, 190(11), 675.
- [51] Das, S., & Sarkar, R. (2019). Predicting the land use and land cover change using Markov model: A catchment level analysis of the Bhagirathi-Hugli River. *Spatial Information Research*, 27, 439-452.
- [52] Cohen, J. (1968). Weighted kappa: Nominal scale agreement provision for scaled disagreement or partial credit. *Psychological bulletin*, 70(4), 213.
- [53] Congalton, R. G., & Green, K. (2019). *Assessing the accuracy of remotely sensed data: principles and practices*. CRC press.
- [54] Alam, N., Saha, S., Gupta, S., & Chakraborty, S. (2021). Prediction modelling of riverine landscape dynamics in the context of sustainable management of floodplain: a Geospatial approach. *Annals of GIS*, 27(3), 299-314.
- [55] Bortle, J. E. (2001). The bortle dark-sky scale. *Sky and Telescope*, 161(126), 5-6.
- [56] Nurhalizza, A., Sutrisno, S., Subiyanto, A., & Hapsoro, C. (2022). Measurement of the quality of the night sky as a feasibility study for astronomy tourism using a sky quality meter at jurang senggani campground, tulungagung regency, east java. *Journal of Physics Conference Series*, 2377(1), 012035.
- [57] Wesolowski, M. (2023). The increase in the surface brightness of the night sky and its importance in visual astronomical observations. *Scientific Reports*, 13(1).
- [58] Şahinoğlu, İ., & Taç, Z. A. (2025). Kentleşme Politika ve Uygulamaları Bağlamında Kentsel Saçaklanma. *Hacettepe Üniversitesi İktisadi ve İdari Bilimler Fakültesi Dergisi*, 43(2), 325-349.
- [59] Öncel, H., & Meşhur, M. Ç. (2021). Konya Kentsel Alanının Büyümesinde Kentsel Saçaklanma ve Nedenleri. *Planlama*, 31(2).
- [60] MEMİŞ, L., DÜZGÜN, S., & KÖSEOĞLU, S. (2023). Covid-19 Salgını, Tersine Göç ve Köy Yerleşimleri: Muhtarlara Yönelik Bir Araştırma. *Amme İdaresi Dergisi*, 56(2).
- [61] Danış, D. (2024). Şubat 2023 Depremleri sonrası toplumsal eşitsizlikler ve göç örüntüleri. *REFLEKTİF Sosyal Bilimler Dergisi*, 5(2), 517-534.
- [62] Karatay, Z. D., & Çilmi, M. (2024). DEPREM SONRASI YAŞANAN ZORUNLU GÖÇ VE İSTİHDAM PROBLEMİ. *Akademik Yaklaşımlar Dergisi*, 15(1-Deprem Özel Sayısı-), 314-333.
- [63] Sezgin, D., & Varol, Ç. (2012). Ankara'daki kentsel büyüme ve saçaklanmanın verimli tarım topraklarının amaç dışı kullanımına etkisi.
- [64] Yavuz, F. (2021). Urban sprawl: An empirical analysis for Konya Province-Turkey. *A/Z ITU J. Fac. Archit*, 18, 79-97.
- [65] Tosun, K. E. (2013). Sürdürülebilir kentsel gelişim sürecinde kompakt kent modelinin analizi. *Dokuz Eylül Üniversitesi Sosyal Bilimler Enstitüsü Dergisi*, 15(1), 103-120.
- [66] Kocaman, Y. (2025). Türkiye'de Demografik Dönüşüm Sürecine Kuramsal Bir Bakış: Temel Nüfus Parametrelerinden Sosyal Sonuçlara. *Senectus*, 3(2), 169-204.
- [67] Gaston, K.J., Visser, M.E. & Hölker, M. (2015). The biological impacts of artificial light at night: the research challenge. *Philosophical Transactions B*, 370, 20140133.

- [68] Ashkenazi, L. & Haim, A. (2012). Light interference as a possible stressor altering HSP70 and its gene expression levels in brain and hepatic tissues of golden spiny mice. *The Journal of Experimental Biology* 215, 4034-4040.
- [69] Grubisic, M., van Grunsven, R.H.A., Kyba, C.C.M., Manfrin, A. & Hölker, F. (2018). Insect declines and agroecosystems: does light pollution matter? *Annals of Applied Biology*, 173, 180–189.
- [70] Jain, M. (2024). Future land use and land cover simulations with cellular automata-based artificial neural network: A case study over delhi megacity (india). *Heliyon*, 10 (14): e34662. Online: <https://doi.org/10.1016/j.heliyon.2024.e34662>.
- [71] Amoakoh, A. O., Aplin, P., Rodríguez-Veiga, P., Moses, C., Alonso, C. P., Cortés, J. A., ... & Nortey, D. D. N. (2024). Predictive Modelling of Land Cover Changes in the Greater Amanzule Peatlands Using Multi-Source Remote Sensing and Machine Learning Techniques. *Remote Sensing*, 16(21), 4013.

